J|A|C|S
ARTICLES
Published on Web 03/21/2003

Discovery of Aminoglycoside Mimetics by NMR-Based Screening of *Escherichia coli* A-site RNA

Liping Yu,* Thorsten K. Oost, Jeffrey M. Schkeryantz,† Jianguo Yang, Dave Janowick,‡ and Stephen W. Fesik

Contribution from the Pharmaceutical Discovery Division, GPRD, Abbott Laboratories, Abbott Park, Illinois 60064-6098

Received November 15, 2002; E-mail: liping.yu@abbott.com

Abstract: A method is described for the NMR-based screening for the discovery of aminoglycoside mimetics that bind to *Escherichia coli* A-site RNA. Although aminoglycosides are clinically useful, they exhibit high nephrotoxicity and ototoxicity, and their overuse has led to the development of resistance to important microbial pathogens. To identify a new series of aminoglycoside mimetics that could potentially overcome the problems associated with toxicities and resistance development observed with the aminoglycosides, we have prepared large quantities of *E. coli* 16 S A-site RNA and conducted an NMR-based screening of our compound library in search for small-molecule RNA binders against this RNA target. From these studies, several classes of compounds were identified as initial hits with binding affinities in the range of 70 μM to 3 mM. Lead optimization through synthetic modifications of these initial hits led to the discovery of several small-molecule aminoglycoside mimetics that are structurally very different from the known aminoglycosides. Structural models of the A-site RNA/ligand complexes were prepared and compared to the three-dimensional structures of the RNA/aminoglycoside complexes.

Introduction

The increasing realization of the essential roles of RNA in many biological processes and in the progression of diseases makes RNA an attractive target in drug discovery. The search for small organic molecules that interact with RNA is therefore drawing growing interest for drug discovery.[1−4] There are many potential RNA targets, including RNA that is involved in cellular protein interactions such as transcription, splicing, and translation, and RNA that is involved in viral infection such as human immunodeficiency virus (HIV) Rev response element (RRE),[5] the trans-activation responsive element (Tar),[6] and the hepatitis C-virus internal ribosome entry site (IRES) RNA.[7] The recently solved crystal structures of the ribosome[8−13] and other cellular and viral RNA motifs[14] open up numerous opportunities for the discovery of small molecules that modulate RNA functions.

One of the most promising RNA targets is the bacterial ribosome 16 S decoding region aminoacyl-tRNA site (A-site) RNA. This RNA target is well validated, since aminoglycoside antibiotics bind to this A-site RNA[15] and cause misreading of the bacterial genetic code, inhibition of translocation, and bacterial cell death.[16,17] Aminoglycosides are effective drugs and widely used in the therapy against bacterial infections.[18] However, aminoglycoside antibiotics display high nephrotoxicity and ototoxicity in the clinic, resulting in kidney failure, hearing loss, and deafness.[19,20] Furthermore, as is the case with virtually all classes of antibiotics, bacterial resistance has been widely developed against this class of antibiotics.[19,21,22]

The structures of the *E. coli* A-site RNA when free and complexed with the antibiotics paromomycin and gentamicin have been determined by NMR and crystallography.[11,23−26] The

† Current address: Eli Lilly and Co., Division of Chemistry Research, Lilly Corporate Center, Indianapolis, IN 46285.
‡ Current address: Pfizer Inc., La Jolla Laboratories, 3550 General Atomics Court, San Diego, CA 92121.

(1) Michael, K.; Tor, Y. *Chem. Eur. J.* **1998**, *4*, 2091.
(2) Afshar, M.; Prescott, C. D.; Varani, G. *Curr. Opin. Biotechnol.* **1999**, *10*, 59.
(3) Gallego, J.; Varani, G. *Acc. Chem. Res.* **2001**, *34*, 836.
(4) Swayze, E. E.; Griffey, R. H. *Expert Opin. Ther. Pat.* **2002**, *12*, 1367.
(5) Zapp, M. L.; Stern, S.; Green, M. R. *Cell* **1993**, *74*, 969.
(6) Wang, S.; Huber, P. W.; Cui, M.; Czarnik, A. W.; Mei, H.-Y. *Biochemistry* **1998**, *37*, 5549.
(7) Le, S.-Y.; Siddiqui, A.; Maizel, J. V., Jr. *Virus Genes* **1996**, *12*, 135.
(8) Ban, N.; Nissen, P.; Hansen, J.; Moore P. B.; Steitz, T. A. *Science* **2000**, *289*, 905.
(9) Brodersen, D. E.; Clemons, W. M., Jr.; Carter, A. P.; Morgan-Warren, R. J.; Wimberly, B. T.; Ramakrishnan, V. *Cell* **2000**, *103*, 1143.
(10) Carter, A. P.; Clemons, W. M.; Brodersen, D. E.; Morgan-Warren, R. J.; Wimberly, B. T.; Ramakrishnan, V. *Nature* **2000**, *407*, 340.
(11) Wimberly, B. T.; Brodersen, D. E.; Clemons, W. M., Jr.; Morgan-Warren, R. J.; Carter, A. P.; Vonrhein, C.; Hartsch, T.; Ramakrishnan, V. *Nature* **2000**, *407*, 327.
(12) Ogle, J. M.; Brodersen, D. E.; Clemons, W. M., Jr.; Tarry, M. J.; Carter, A. P.; Ramakrishnan, V. *Science* **2001**, *292*, 897.
(13) Yusupov, M. M.; Yusupova, G. Z.; Baucom, A.; Lieberman, K.; Earnest, T. N.; Cate, J. H. D.; Noller, H. F. *Science* **2001**, *292*, 883.
(14) Lukavsky, P. J.; Otto, G. A.; Lancaster, A. M.; Sarnow, P.; Puglisi, J. D. *Nature Struct. Biol.* **2000**, *7*, 1105.
(15) Fourmy, D.; Recht, M. I.; Puglisi, J. D. *J. Mol. Biol.* **1998**, *277*, 347.
(16) Noller, H. F. *Annu. Rev. Biochem.* **1991**, *60*, 191.
(17) McGowan, J. P. *Cancer Invest.* **1998**, *16*, 528.
(18) Begg, E. J.; Barclay, M. L. *Br. J. Clin. Pharmacol.* **1995**, *39*, 597.
(19) Spelman, D. W.; McDonald, M.; Spicer, W. J. *Med. J. Aust.* **1989**, *151*, 346.
(20) Slaughter, R. L.; Cappelletty, D. M. *Pharmacoeconomics* **1998**, *14*, 385.
(21) Zembower, T. R.; Noskin, G. A.; Postelnick, M. J.; Nguyen, C.; Peterson, L. R. *Int. J. Antimicrob. Agents* **1998**, *10*, 95.
(22) Haddad, J.; Vakulenko, S.; Mobashery, S. *J. Am. Chem. Soc.* **1999**, *121*, 11922.
(23) Fourmy, D.; Recht, M. I.; Blanchard, S. C.; Puglisi, J. D. *Science* **1996**, *274*, 1367.
(24) Fourmy, D.; Yoshizawa, S.; Puglisi, J. D. *J. Mol. Biol.* **1998**, *277*, 333.
(25) Yoshizawa, S.; Fourmy, D.; Puglisi, J. D. *EMBO J.* **1998**, *17*, 6437.

10.1021/ja021354o CCC: $25.00

aminoglycosides bind to the pocket formed by the residues located in the internal loop. The complex formation is stabilized by a combination of intermolecular hydrogen bonds and electrostatic and hydrophobic interactions. Previous studies have primarily centered on chemical modifications of known aminoglycosides for the improvement of their antibiotic properties.[27−31] The goal of this study is to discover small molecules that bind to the A-site RNA that could serve as aminoglycoside mimetics. These compounds may exhibit less toxicity and may be effective against bacteria that are resistant to aminoglycosides and other classes of antibiotics. There are several methods that could be used to identify ligands for the A-site RNA. One approach is the mass-spectrometry-based screening of RNA as recently described for the 23 S rRNA target.[32,33] Another approach utilizes a fluorescently labeled aminoglycoside as a probe to discover competitive binders.[34] Alternatively, surface plasmon resonance (SPR) could be employed to detect ligand binding to RNA by monitoring changes in the optical properties of the surface when ligands bind to immobilized RNA molecules.[28,35]

Here, we describe an NMR-based screening approach to identify ligands that bind to RNA. This approach has the advantages of identifying not only ligands that bind to RNA but also the RNA residues that are perturbed by the binding of the ligands simultaneously. However, this approach requires relatively large amounts of RNA. To prepare large quantities of *E. coli* A-site RNA for the NMR-based screening, we used a ribozyme approach that generates a high yield of transcriptional RNA and easy separation of the targeted RNA. The purified *E. coli* A-site RNA was then used in the NMR-based screening of our compound library that contains ~10 000 compounds. The screening hit rate is about 3%. This approach led to the discovery of several novel series of RNA-binding ligands that were structurally very different from the known aminoglycosides.

Results and Discussion

Preparation of Large Quantities of RNA. To apply NMR-based screening to the *E. coli* A-site RNA, a key requisition was to prepare large quantities of RNA. The RNA sequence used in this study is shown in Figure 1. The *E. coli* A-site RNA corresponds to the sequence inside the box. The additional three base pairs at the top were introduced to stabilize the top base stem, while a four-base loop at the bottom was constructed to connect the two RNA strands.

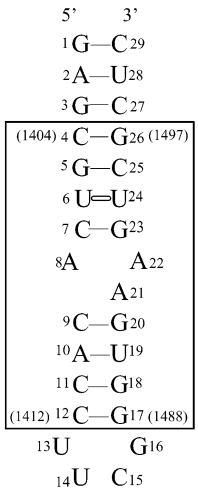

Figure 1. RNA sequence of the A-site oligonucleotide used in the current studies. The sequence inside the box corresponds to the decoding region of *E. coli* 16 S A-site rRNA. The sequence numbers of the *E. coli* 16 S rRNA are indicated in parentheses.

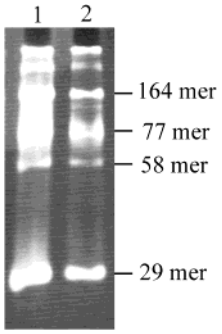

Figure 2. Representative gels of the optimized transcription reaction products are shown in lanes 1 and 2. The gels were stained with ethidium bromide. Lanes 1 and 2 were loaded with 2 and 1 μL of the transcription products. The bands on the gel correspond to the cleaved target *E. coli* A-site RNA (29-mer), 5′-hammerhead ribozyme 1 (58-mer), and 3′-hammerhead ribozyme 2 (77-mer), as well as the uncleaved transcription product (164-mer). Some other bands around 77-mer correspond to the partially cleaved products. Even for the overloaded lane 1, the target 29-mer RNA is still well resolved from the other RNA molecules. Thus, it can be easily separated.

We have adopted the method that uses cis-acting hammerhead ribozyme flanking at both the 5′ and 3′ ends of the target RNA sequence for large-scale RNA production.[36] There are two advantages of this method over the traditional transcriptional runoff reaction. First, higher yields of RNA can be obtained, since the optimal sequence can be used at the 5′ end of the hammerhead ribozyme. Second, a clean cut can be obtained at both the 5′ and 3′ ends of the target sequence. In contrast, when using the traditional transcriptional runoff reaction,[37] the 3′ end of the RNA sequence usually is heterogeneous (with n and $n \pm 1$ lengths). The separation of the n and $n \pm 1$ bands is very difficult, especially when purifying large quantities of target RNA. However, with this approach, it is now much easier to separate the cleaved target RNA from the hammerhead ribozymes, which have very different sizes compared to the 29-mer target RNA (Figure 2). A similar approach has been reported by using different ribozymes for cleavage.[38] Small-

(26) Lynch, S.; Puglisi, J. D. *J. Mol. Biol.* **2001**, *306*, 1037.
(27) (a) Wang, H.; Tor, Y. *Bioorg. Med. Chem. Lett.* **1997**, *7*, 1951. (b) Simonsen, K. B.; Ayida, B. K.; Vourloumis, D.; Takahashi, M.; Winters, G. C.; Barluenga, S.; Qamar, S.; Shandrick, S.; Zhao, Q.; Hermann, T. *ChemBioChem* **2002**, *3*, 1223. (c) Vourloumis, D.; Takahashi, M.; Winters, G. C.; Simonsen, K. B.; Ayida, B. K.; Barluenga, S.; Qamar, S.; Shandrick, S.; Zhao, Q.; Hermann, T. *Bioorg. Med. Chem. Lett.* **2002**, *12*, 3367.
(28) Wong, C.-H.; Hendrix, M.; Manning, D. D.; Rosenbohm, C.; Greenberg, W. A. *J. Am. Chem. Soc.* **1998**, *120*, 8319.
(29) Alper, P. B.; Hendrix, M.; Sears, P.; Wong, C.-H. *J. Am. Chem. Soc.* **1998**, *120*, 1965.
(30) Sucheck, S. J.; Wong, A. L.; Koeller, K. M.; Boehr, D. D.; Draker, K.-A.; Sears, P.; Wright, G. D.; Wong, C.-H. *J. Am. Chem. Soc.* **2000**, *122*, 5230.
(31) Sucheck, S. J.; Greenberg, W. A.; Tolbert, T. J.; Wong, C.-H. *Angew. Chem., Int. Ed.* **2000**, *39*, 1080.
(32) Swayze, E. E.; Jefferson, E. A.; Sannes-Lowery, K. A.; Blyn, L. B.; Risen, L. M.; Arakawa, S.; Osgood, S. A.; Hofstadler, S. A.; Griffey, R. H. *J. Med. Chem.* **2002**, *45*, 3816.
(33) Griffey, R. H.; Hofstadler, S. A.; Sannes-Lowery, K. A.; Ecker, D. J. *Proc. Natl. Acad. Sci. U.S.A.* **1999**, *96*, 10129.
(34) Tok, J. B.-H.; Rando, R. R. *J. Am. Chem. Soc.* **1998**, *120*, 8279.
(35) Hendrix, M.; Priestley, E. S.; Joyce, G. F.; Wong, C.-H. *J. Am. Chem. Soc.* **1997**, *119*, 3641.
(36) Price, S. R.; Ito, N.; Oubridge, C.; Avis, J. M.; Nagai, K. *J. Mol. Biol.* **1995**, *249*, 398.
(37) Milligan, J. F.; Groebe, D. R.; Witherell, G. W.; Uhlenbeck, O. C. *Nucleic Acids Res.* **1987**, *15*, 8783.

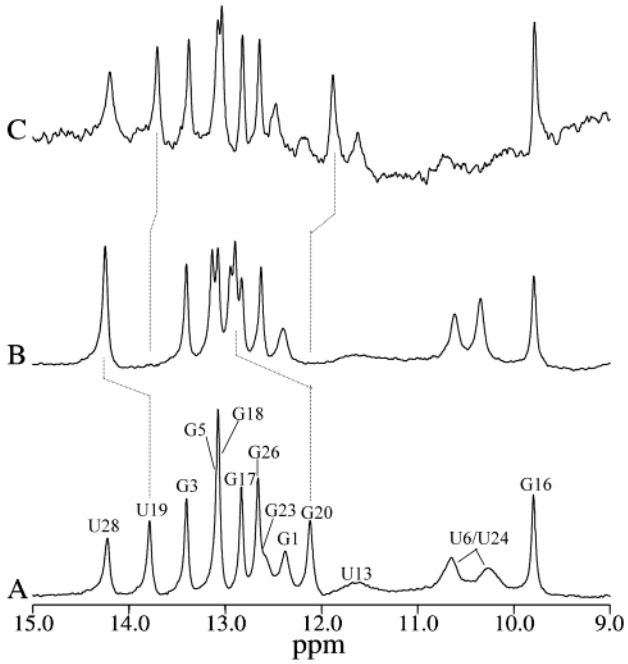

Figure 3. 1D ^{1}H spectra of the imino region of the RNA molecule at 25 °C: (A) free RNA; (B) RNA in the presence of paromomycin (1:1 ratio); (C) typical ^{1}H spectrum of the RNA in the presence of library compounds that bind to this piece of RNA (compound **1** in this case at 1.0 mM). The assignments for the imino protons of the RNA are indicated for the free RNA.

scale transcription reactions were usually carried out before a large batch preparation was undertaken in order to optimize the buffer components, the NTP concentrations, and the amount of DNA template and T7 RNA polymerase in the transcription reaction. We typically obtained 0.8 mg of purified A-site RNA per mL transcription reaction. The RNA products from a typical transcription reaction are shown in Figure 2.

The RNA sequence used in this study is identical to that reported previously[39] except that one additional base pair AU was inserted into the top base stem which is not part of the *E. coli* A-site RNA sequence. This insertion was designed such that the cis-acting 3′ hammerhead ribozyme could cleave the target RNA at the 3′ end of the target sequence. The purified RNA binds tightly to paromomycin, as evidenced by the dramatic shift of the imino protons of U19 and G20 (Figure 3B), which is in good agreement with the results previously described.[39]

Identification of Ligands That Bind to the 29-mer RNA. The imino proton region of the 29-mer RNA is well resolved and easily assigned from 2D NOESY experiments (Figure 3A). Therefore, the imino proton region of one-dimensional NMR spectra was used to monitor the spectral changes upon the addition of compounds for the identification of ligands that bind to this RNA target. The screening protocol that was employed in this study is similar to that published previously for screening protein targets.[40,41] First, mixtures of 10 compounds (at 0.5 mM each) were added to a 50 μM solution of 29-mer RNA in 20 mM sodium phosphate with a final DMSO concentration of 0.5%. The ^{1}H NMR spectrum of the imino proton region of the

Table 1. Dissociation Constants for Members of the 2-Aminobenzimidazole Series that Bind to the Aminoglycoside-Binding Pocket of the *E. coli* A-site RNA

Compound No.	Compounds	K_d (mM)[a]
1	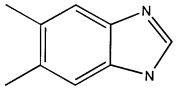	0.81
2	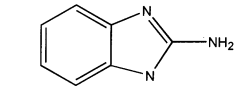	0.23
3	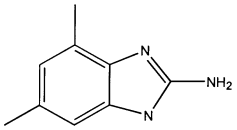	0.26
4	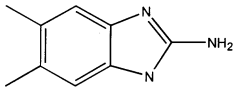	0.22
5	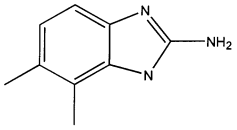	0.16

[a] Dissociation constants were derived from an analysis of the changes in the imino proton chemical shifts as a function of compound concentration. The errors in the dissociation constants are ~16% as estimated by using a Monte Carlo simulation as previously described.[41]

RNA in the presence of compounds was collected and compared with the corresponding spectrum of the free RNA. If changes in chemical shifts were observed, the compounds in this mixture were tested individually in order to identify the compound responsible for causing the changes in chemical shifts. We screened about 10 000 compounds from our compound library. A representative ^{1}H NMR spectrum of the RNA in the presence of representative screening hit **1** (Table 1) is shown in Figure 3C, where the imino protons of G20, G23, and U19 are clearly shifted. The RNA binding affinities (K_d) were determined by fitting the chemical shift data as a function of ligand concentration as described previously.[41] Representative fits are shown in Figure 4. Since the imino protons of this RNA are well resolved, usually very selective changes in the NMR spectra were observed for the RNA binders. The resolved G20 imino proton oftentimes was monitored for the K_d measurements, since it was one of the most perturbed peaks upon ligand binding and had a reasonably narrow line width. We typically collected 6 data points in the titration for the K_d measurements. Ligand binding to RNA could also be detected by a saturation transfer difference (STD) experiment as recently described.[42]

From NMR-based screening, several classes of compounds were identified that bind to this RNA molecule (Tables 1 and 2). Benzimidazole derivatives in Table 1 were found to bind in

(38) Ferre-D'Amare, A. R.; Doudna, J. A. *Nucleic Acids Res.* **1996**, *24*, 977.
(39) Recht, M. I.; Fourmy, D.; Blanchard, S. C.; Dahlquist, K. D.; Puglisi, J. D. *J. Mol. Biol.* **1996**, *262*, 421.
(40) Shuker, S. B.; Hajduk, P. J.; Meadows, R. P.; Fesik, S. W. *Science* **1996**, *274*, 1531.
(41) Hajduk, P. J.; Sheppard, G.; Nettesheim, D. G.; Olejniczak, E. T.; Shuker, S. B.; Meadows, R. P.; Steinman, D. H.; Carrera, G. M., Jr.; Marcotte, P. A.; Severin, J.; Walter, K.; Smith, H.; Gubbins, E.; Simmer, R.; Holzman, T. F.; Morgan, D. W.; Davidsen, S. K.; Summers, J. B.; Fesik, S. W. *J. Am. Chem. Soc.* **1997**, *119*, 5818.
(42) Mayer, M.; James, T. L. *J. Am. Chem. Soc.* **2002**, *124*, 13376.

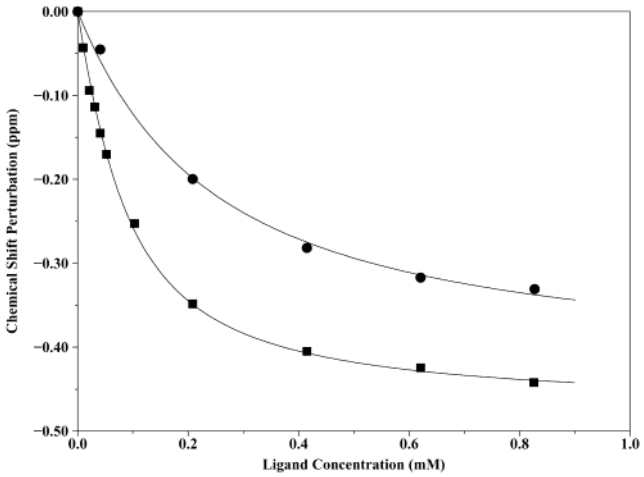

Figure 4. Representative fits of the chemical shift of the imino proton of the ligand-binding pocket nucleotide G20 as a function of ligand concentration. The chemical shift perturbation is the chemical shift difference ($\delta_{bound} - \delta_{free}$) of the RNA. The fitted RNA-binding affinities (K_d) are 60 μM for compound **11** (filled square) and 220 μM for compound **4** (filled circle).

Table 2. Dissociation Constants for Members of the 2-Aminoquinoline Series that Bind to the Aminoglycoside-Binding Pocket of the *E. coli* A-site RNA

Compound No.	Compounds	K_d (mM)[a]
6	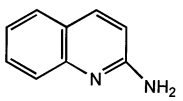	3.18
7	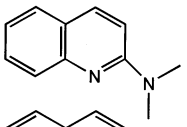	0.99
8	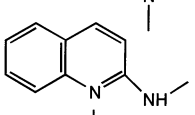	0.49
9	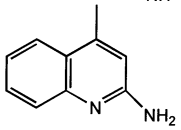	0.09
10	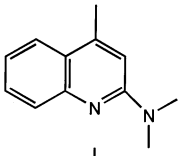	0.17
11	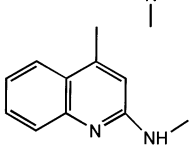	0.06

[a] Dissociation constants were derived from an analysis of the changes in the imino proton chemical shifts as a function of compound concentration. Based on the pK_a calculation with the ACD software, the methyl substitution at the position 4 increased the pK_a by 0.57, while the mono- and dimethyl substitution at the 2-amino position increased pK_a by 0.33 and 0.28, respectively. The increase in pK_a values is correlated with the increase in RNA binding affinity.

the submillimolar range. In this series, 2-amino substitution led to a 4-fold increase in binding affinity (compound **1** vs **4**). Methyl substituents on the phenyl portion had little effect on the binding affinity (compound **2** vs **3**−**5**). 2-Aminoquinolines

Table 3. Dissociation Constants for Analogues of the 2-Aminoquinoline Lead that Bind to the Aminoglycoside-Binding Pocket of the *E. coli* A-site RNA

Compound No.	Compounds	K_d (mM)[a]
12	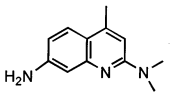	0.035
13	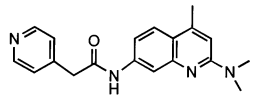	0.018
14	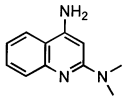	0.060
15	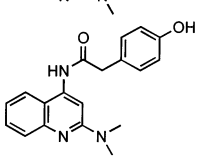	0.009 ± 0.005[b]

[a] Dissociation constants were derived from an analysis of the changes in the imino proton chemical shifts as a function of compound concentration. [b] Standard deviation was obtained from duplicate measurements.

6−**10** were found to bind the RNA with affinities ranging from ~90 μM to 3.2 mM (Table 2). In this series, the 2-methylamine analogue **8** was found to bind more tightly than the 2-amino and 2-dimethylamino analogues (**6**, **7**). 4-Methyl substitution (2-aminolepidine series) led to a large increase in binding affinity (compounds **6** vs **9**, and **7** vs **10**). These observations prompted us to synthesize 2-(methylamino)lepidine (**11**). By combining the methyl substitutions at the 2-amino and 4 positions, which individually exhibited improved affinity, the highest affinity analogue **11** in this series was produced (K_d of 60 μM).

The 1D screening method employed in the current study is simple and fast and does not require ^{15}N- or ^{13}C-labeling of RNA. This method is applicable to any RNA targets in which the imino proton region can be resolved. For larger RNA targets in which the imino protons are severely overlapped, the screening could be carried out by using ^{15}N- (and/or ^{13}C)-labeled RNA and by collecting 2D HSQC spectra, which would significantly reduce the spectral overlap.

Further Optimization of the 2-Aminoquinoline Lead. The 2-aminoquinoline lead was chosen for further optimization. On the basis of structural information derived from NMR data as well as from ligand docking using molecular models of the RNA/ligand complexes, we envisioned that the 4- and 7-position of the 2-aminoquinoline scaffold could provide vectors toward additional RNA pockets that are occupied by paromomycin. According to the previously published synthetic protocols,[43,44] 7-amino-2-dimethylaminolepidine (**12**) and 4-amino-2-dimethylaminoquinoline (**14**) were prepared. Both compounds can readily be derivatized via their amino moiety. We found that the parent amines (**12** and **14**) have increased binding affinities when compared to the desamino analogues (**10** and **7**) (Tables 2 and 3). In a parallel synthesis approach, numerous amide, urea, and carbamate analogues were prepared starting from the core intermediates **12** and **14**. Amides **13** and **15** represent active

(43) Nasr, M.; Drach, J. C.; Smith, S. H.; Shipman, C.; Burckhalter, J. H. *J. Med. Chem.* **1988**, *31*, 1347.
(44) Eiden, F.; Berndl, K. *Arch. Pharm. (Weinheim, Ger.)* **1986**, *319*, 347.

Table 4. Dissociation Constants for Members of the 2-Aminopyridine Series that Bind to the Aminoglycoside-Binding Pocket of the *E. coli* A-site RNA

Compound No.	Compounds	K_d (mM)[a]
16	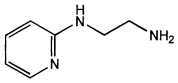	0.068
17	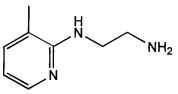	0.600
18	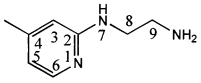	0.003 ± 0.001[b]
19	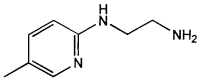	0.022 ± 0.008[b]
20	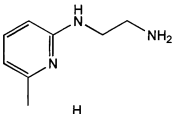	0.105
21	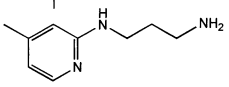	0.020 ± 0.012[b]
22	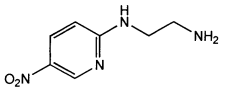	> 10

[a] Dissociation constants were derived from an analysis of the changes in the imino proton chemical shifts as a function of compound concentration. [b] Standard deviations were obtained from duplicate measurements.

library members. Compared to the parent amines, they exhibit improved RNA binding affinities with K_d values of 18 and 9 μM, respectively (Table 3).

Optimization of the 2-Aminopyridine Lead. During the initial NMR-based screening, 2-aminopyridine **16** was found to bind to the *E. coli* A-site RNA with an affinity of 68 μM (Table 4). This screening hit was attractive, since it is even smaller than the previously discovered 2-aminoquinolines and yet binds to the RNA with good affinity. Therefore, a series of analogues was prepared to test whether the RNA binding affinity of this hit can be further improved. A systematic "methyl scan" of the pyridine ring revealed an interesting structure−activity relationship. The 3- and 6-methyl substitutions (**17** and **20**) led to decreased binding, whereas, the 4- and 5-substitutions (**18** and **19**) resulted in an improved affinity. The 4-methyl analogue **18** was the tightest binder in this series, with a K_d of 3 μM, which represents a 22-fold improvement over the parent compound **16**. Interestingly, we had observed a similar increase in binding affinity earlier when we switched from the 2-aminoquinoline to the 2-aminolepidine series (Table 2, e.g., compound **8** vs **11**). The homologous analogue **21**, with an (aminopropyl)-amino side chain, was also found to bind to the RNA with good affinity. Analogues with an electron-withdrawing 5-nitro substituent (**22**) were devoid of binding affinity, which may be attributed to the significantly reduced basicity of the 2-aminopyridine moiety.

Competition Experiments. The antibiotic neamine is known to bind the *E. coli* A-site RNA[15] with a K_d of ~8 μM based on our NMR titration. Neamine consists of rings I and II of paromomycin[39] and binds to the RNA in two conformations with the ring I either occupying the same position as in the

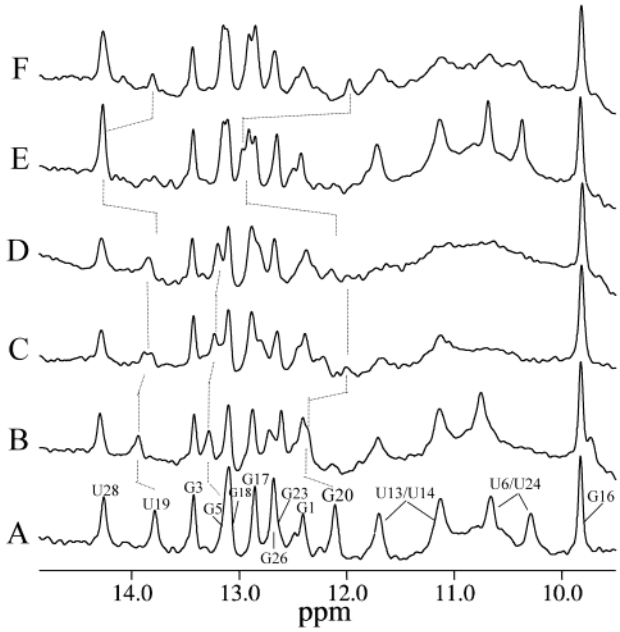

Figure 5. 1D ^{1}H spectra of the imino region of the RNA molecule at 20 °C: (A) 80 μM free RNA (sample A); (B) sample A plus 110 μM neamine (sample B); (C) sample B plus 110 μM compound **18**; (D) sample B plus 220 μM compound **18**; (E) sample A plus 80 μM paromomycin (sample E); (F) sample E plus 160 μM compound **18**. The assignments for the imino protons of the RNA are indicated for the free RNA.

paromomycin complex or in a flipped up orientation occupying the space above ring II near G5 nucleotide.[15] The binding of neamine to the RNA caused a shift of imino proton peaks of U19, G5, G20, and U6/U24 (Figure 5B), which is consistent with the reported structural data.[15] Addition of compound **18** to the RNA/neamine complex caused a shift reversal of the imino protons of U19, G5, and G20, indicating that compound **18** competes with the binding of neamine (Figure 5C,D). Similarly, the binding of paromomycin caused major chemical shifts of the imino protons of U19 and G20 (Figure 5E). This shift pattern is identical to that previously reported.[15,39] Addition of compound **18** to the RNA/paromomycin complex partially displaced paromomycin, as indicated by the presence of a new set of peaks of U19 and G20 (Figure 5F) when compared to Figure 5E. Further addition of compound **18** caused line-broadening of the peaks. These results provide additional evidence that compound **18** binds to the paromomycin-binding site.

It is interesting to note that the U13/U14 and U6/U24 imino peaks are severely broadened in the presence of compound **18** and neamine or paromomycin. These uridine imino peaks are generally broader than the rest of the imino protons (see Figure 3A), and their line widths are sensitive to sample temperature. When compound **18** alone was titrated into the RNA, the U6/U24 and G20 imino protons had very large chemical shift perturbations, while the U13/U14 and G16 imino protons experienced no chemical shift changes. Therefore, we are convinced that compound **18** primarily binds to the paromomycin-binding pocket where these perturbed residues are located. Chemical exchange could have caused the broadening of these uridine imino peaks in the presence of multiple ligands at relatively high concentrations.

Molecular Modeling of the 29-mer RNA/Ligand 18 Complex. To provide information on how compound **18** binds

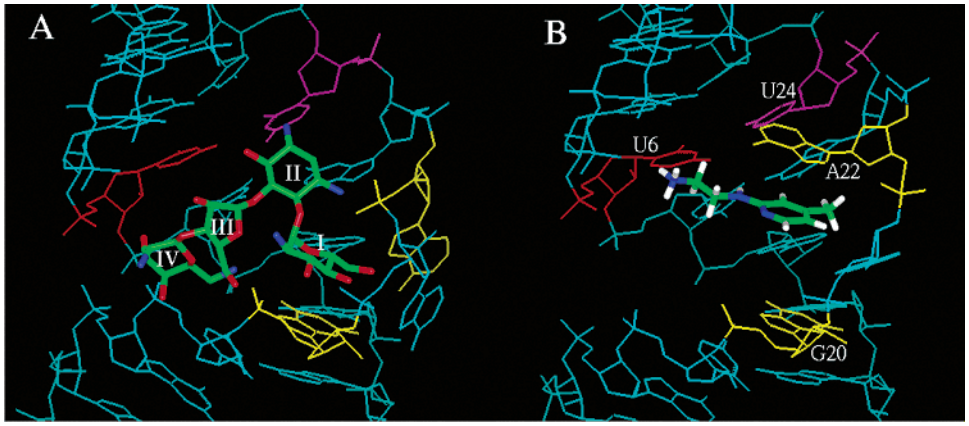

Figure 6. Structure of the *E. coli* A-site RNA in complex with paromomycin (A). Structural model of the lead compound **18** when bound to the aminoglycoside-binding pocket of the *E. coli* A-site RNA (B). The four subunits (I−IV) of paromomycin are labeled in A. Nucleotides G20 and A22 are colored in yellow. Nucleotides U6 and U24 are colored in red and magenta, respectively.

Table 5. Intermolecular NOEs Observed between 29-mer RNA and Compound **18** at a Mixing Time of 150 ms

Protons on Ligand **18**	Protons on 29-mer RNA	Relative NOE Intensity
4-methyl	A22 H8	medium
4-methyl	A21 H8	medium
H5	A22 H8	weak
H5	A21 H8	weak
H3	A22 H2	weak
H9a	U6 H5	strong
H9b	U6 H5	strong

to the A-site RNA, NOE experiments were performed. A total of seven intermolecular NOEs were obtained for the 29-mer RNA/compound **18** complex at a mixing time of 150 ms (Table 5). Although this small number of intermolecular NOEs was insufficient to calculate well-resolved structures of this complex, they did allow a model of the complex to be prepared (Figure 6B).

The model was generated by docking **18** into the free *E. coli* A-site RNA structure previously determined by Puglisi and coworkers,[24] and the docking was guided by the observed intermolecular NOE restraints (Table 5). The NOEs observed between the compound pyridine ring 4-methyl and H5 protons (see compound **18** atom numbering in Table 4) and the RNA A21 and A22 H8 protons place this pyridine ring near a location that is occupied by rings I and II of paromomycin (Figure 6A). The compound pyridine ring stacks above the base G20 and against the base of A21. The observed NOEs between A22 H2 and U24 H5 indicate that the base of A22 has rotated toward the inside of the ligand-binding pocket and stacks on the top of the compound pyridine ring. This ligand and RNA base stacking is consistent with the observed intermolecular NOEs between A22 H2 and compound pyridine H3 and between A22 H8 and pyridine 4-methyl and H5. The side-chain off the 2-amino pyridine ring of compound **18** points toward the base of U6. This is evidenced by the strong NOEs observed between the ligand H9 methylene protons and RNA U6 H5, but not between the ligand H8 methylene protons and RNA U6 H5. On the basis of the model, the positively charged terminal NH_3 group of the ligand is positioned to form an electrostatic interaction with the negatively charged phosphate of G5. The ligand NH (H7) likely forms hydrogen bonds with G23 O6 and/or U6 O4. This binding mode is also consistent with the significantly reduced binding of compound **17** in which the 3-methyl substitution could cause steric hindrance and prevent the formation of these hydrogen bonds.

Conclusions. To address the problems associated with toxicity and development of resistance against aminoglycoside antibiotics, we chose the *E. coli* A-site RNA as a target and screened for small molecules that bind to this site and that could potentially be developed into novel aminoglycoside mimetics. Large quantities of *E. coli* A-site RNA were generated for the NMR-based screening and NMR-based structural studies using a bis-ribozyme construct. High-throughput NMR-based screening of our compound library delivered several series of initial hits that were further optimized. This led to the rapid discovery of small-molecule RNA binders that bind to the target RNA in the single digit micromolar range.

Aminoglycosides are known to bind to many different RNA targets. For example, the aminoglycoside neomycin binds to the prokaryotic 16 S A-site RNA, group I intron RNA, HIV TAR element, and hammerhead ribozyme.[5,6,15,45] Therefore, the binding of the aminoglycosides to RNAs is not very specific. The compounds discovered from the current study likely also bind to other RNA targets, although they may exhibit different binding affinities. With the rapidly expanding knowledge of the three-dimensional structures of RNA/ligand complexes and the better understanding of RNA dynamics, it may be possible to design specific RNA inhibitors through the use of maximized shape and electrostatic complementarity and hydrogen-bond formation. The leads from this study could serve as novel templates, which can be further developed into possible replacements for the aminoglycoside antibiotics, which suffer from toxicity and resistance development.

Experimental Section

Preparation of *E. coli* A-Site Oligonucleotide RNA. The DNA sequences of the T7 promoter (ATAATACGACTCACTATA), 58-mer 5′-hammerhead ribozyme 1 (GGGAGAGTGTGACGCTCCTGATGAGTCCGTGAGGACGAAACGGTATCTAGATACCGTC), 29-mer target RNA (GAGCGTCACACCTTCGGGTGAAGTCGCTC), and 77-mer 3′-hammerhead ribozyme 2 (GACGGAGTCTAGACTCCGTCCTGATGAGTCCGTGAGGACGAAAGCGACTAAATAAACCAACTGCCGGCATGCAAGCT) were cloned into pUC18 vector with an EcoR I cleavage site at the 5′ end and Hind III cleavage site at the 3′

(45) (a) von Ahsen, U.; Davies, J.; Schroeder, R. *J. Mol. Biol.* **1992**, *226*, 935. (b) Hermann, T.; Westhof, E. *J. Mol. Biol.* **1998**, *276*, 903.

end of the DNA sequence. The vector was then transformed into a DH5α cell, and its inserted DNA sequence was confirmed from sequencing gels. After growing a large batch of the transformed cells, the plasmid DNA was isolated with Maxi or Mega kits from Qiagen. Subsequently, the purified plasmid DNA was linearized through cutting with Hind III restriction enzyme and further purified with phenol/CH_3Cl extraction. The linearized DNA was then used as a template in the in vitro transcription reaction.

The in vitro transcription reaction was carried out in a transcription buffer typically containing 40 mM Tris-HCl (pH 7.9), 2 mM spermidine, 40 mM $MgCl_2$, 10 mM NaCl, 10 mM DTT, 21.2 mM NTP (4.0 mM UTP, 5.3 mM CTP, 5.5 mM ATP, and 6.4 mM GTP, which are optimized based upon the nucleotide composition of the transcribed sequence), plasmid DNA template 28 nM, 0.05% Triton-X100, and T7 RNA polymerase 2000 units/mL reaction. The amount of $MgCl_2$ needed in the transcription buffer is very sensitive to the amount of NTP present as well as how the NTPs were prepared. For instance, the in-house-prepared ^{13}C- and ^{15}N-labeled NTPs may already contain a significant amount of Mg^{2+}. Thus, much less $MgCl_2$ was added in the transcription buffer. The T7 RNA polymerase was expressed and purified from a N-terminal His-tagged version of this protein. The products from the in vitro transcription reaction were separated from 20% (w/v) polyacrylamide (29:1 (w/w) acrylamide:bis)/7 M urea gels. The unlabeled RNA was obtained by using unlabeled NTPs purchased from Sigma, and [^{15}N,^{13}C]-doubly labeled RNA was synthesized in the in vitro transcription reaction by employing [^{15}N,^{13}C]-doubly labeled NTPs prepared as previously described.[46,47]

Detection of Ligand Binding. Ligand binding was detected by acquiring 1D spectra with the jump-return method[48] using a 500 μL sample of 50 μM *E. coli* A-site RNA in 20 mM sodium phosphate (pH 6.5) in the presence and absence of added compound. Compounds were added as solutions in perdeuerated DMSO or in aqueous buffer of 20 mM sodium phosphate (pH 6.5). We screened about 10 000 compounds from our compound library. Compounds were initially tested at 0.5 mM each, and binding was determined by monitoring changes in the imino proton region of the 1D ^1H spectra. Dissociation constants were obtained by fitting the chemical shift as a function of ligand concentration through a least-squares grid search by varying the values of dissociation constant K_d and the chemical shift of the fully saturated RNA.[41] For several selected compounds, duplicate experiments were carried out by using 40 μM RNA samples, and their average K_d values and standard deviations were reported.

NMR Spectroscopy. All NMR spectra were collected on a Bruker DRX500, DRX600, or DRX800 NMR spectrometer at 25 °C or otherwise specified temperature. Pulsed field gradients were applied where appropriate as described to afford suppression of solvent signal and spectral artifacts. 1D spectra for the samples in water were acquired with the jump-return method.[48] RNA/ligand complexes were assigned from COSY, TOCSY, and NOESY spectra.[49] The data were processed and analyzed on Silicon Graphics computers using in-house written software.

Molecular Modeling. To provide information on how compound **18** binds to the A-site RNA, compound **18** was titrated into the RNA with increasing compound concentrations, and a series of TOCSY and NOESY spectra with different mixing times were collected at 35 °C at each ligand concentration. This allowed us to trace the cross-peaks that were shifted upon the addition of the compound. On the basis of the published assignments of the free A-site RNA by Puglisi and co-workers,[24] these perturbed peaks/residues were shown to be located in the paromomycin-binding pocket. Seven intermolecular NOEs were observed at mixing time 150 ms (Table 5). Additional intermolecular NOEs between ligand H8 and H9 methylene protons and A22 H2 and between ligand H6 and A22 H8 and A21 H8 were also observed at mixing times of 200 and 300 ms.

Ligand **18** was docked into the free A-site *E. coli* RNA structure that was previously determined by Puglisi and co-workers.[24] The docking was guided by the NMR-derived NOE restraints with the InsightII program. No solvent and sodium counterions were added, and no electrostatic potential was used in the docking. On the basis of the observed NOE connectivity between A22 H2 and U24 H5, the nucleotide 22 was rotated along the phosphate backbone toward the inside of the binding pocket from the initial structure and the RNA structure was then energy-minimized. As a result of this rotation, the base of A22 stacks against the ligand pyridine ring, which is consistent with the observed intermolecular NOEs. During the NOE assignments, it is observed that, at a low ratio of compound to RNA, A22 H2 has NOEs to both U24 H5 and G23 H1′, indicating that the base of A22 has a mixture of free and ligand-bound conformations. Either using NMR samples that contain higher ligand to RNA ratio or lowering experimental temperature drives the RNA to the complete bound conformation.

Supporting Information Available: Experimental procedures and spectral characterization for the compounds described in the text. This material is available free of charge via the Internet at http://pubs.acs.org.

JA021354O

(46) Nikonowicz, E. P.; Sirr, A.; Legault, P.; Jucker, F. M.; Baer, L. M.; Pardi, A. *Nucleic Acids Res.* **1992**, *20*, 4507.
(47) Batey, R. T.; Battiste, J. L.; Williamson, J. R. *Methods Enzymol.* **1995**, *261*, 300.
(48) Plateau, P.; Gueron, M. *J. Am. Chem. Soc.* **1982**, *104*, 7310.
(49) Wüthrich, K. *NMR of Proteins and Nucleic Acids*; John Wiley & Sons: New York, 1986.